

SCIM: Simultaneous Clustering, Inference, and Mapping for Open-World Semantic Scene Understanding

Hermann Blum¹, Marcus G Müller^{1,2}, Abel Gawel³, Roland Siegwart¹,
and Cesar Cadena¹

¹ Autonomous Systems Lab, ETH Zürich, Switzerland

² German Aerospace Center (DLR), Munich, Germany

³ Huawei Research, Zürich, Switzerland

Abstract. In order to operate in human environments, a robot’s semantic perception has to overcome open-world challenges such as novel objects and domain gaps. Autonomous deployment to such environments therefore requires robots to update their knowledge and learn without supervision. We investigate how a robot can autonomously discover novel semantic classes and improve accuracy on known classes when exploring an unknown environment. To this end, we develop a general framework for mapping and clustering that we then use to generate a self-supervised learning signal to update a semantic segmentation model. In particular, we show how clustering parameters can be optimized during deployment and that fusion of multiple observation modalities improves novel object discovery compared to prior work. Models, data, and implementations can be found at github.com/hermannsblum/scim.

Keywords: self-supervised learning, semantic segmentation, self-improving perception, semantic scene understanding

1 Introduction

Robots that automate tasks such as household work, hospital logistics, assistive care, or construction work have to operate in environments that are primarily designed for humans. Moreover, all these tasks have a high level of complexity that requires semantic scene understanding [1]. Semantics in human environments are open-world. They have domain gaps, contain novel objects, and change over time. For robots to operate autonomously in such environments, they need to be able to deal with such changes and novelties. This requires a methodological shift from deploying models trained on fixed datasets to enabling robots to learn by themselves, building up on advancements in self-supervised learning and continual learning. It is the robotic version of ideas like ‘learning on the job’ [2],

This paper was financially supported by the HILTI Group.

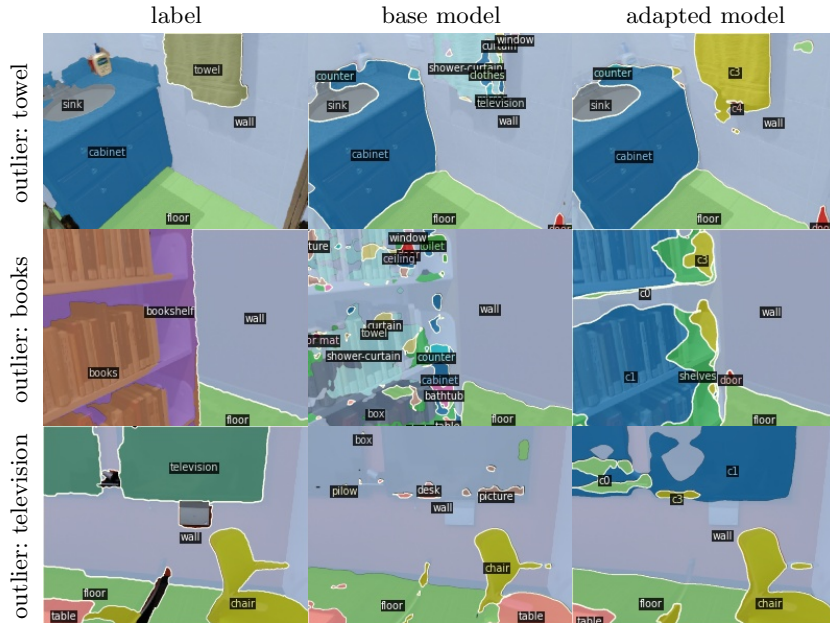


Fig. 1: Example predictions from a segmentation network trained with our method (third column), compared to the predictions of a pretrained model (second column) and the ground-truth label (first column). The base model did not see the outlier class during training. These novel objects are discovered autonomously, and are therefore not labelled by a word but by their cluster id (e.g., c1, c2, ...).

open-world object detection [3] or segmentation [4], and is related to the idea of developmental robotics [5].

This work investigates scenarios where robots should perform semantic scene understanding in unknown environments that contain novel object categories. We show how robots can improve their semantic segmentation in these new environments on both known and unknown categories by leveraging semantic mapping, uncertainty estimation, self-supervision, and clustering. We call the investigated problem ‘Simultaneous Clustering, Inference, and Mapping’ (SCIM). The approaches we investigate work fully autonomously without human supervision or intervention. While fusion of predictions and discovery of novel objects has also been investigated in the context of semantic mapping [6], [7], maps are always bound to one point in time and one specific environment. Instead, segmentation networks can carry knowledge into different environments. Prior work has shown that combining self-supervised pseudo-labels with continual learning can integrate knowledge gathered over multiple environments in closed-world [8], which would not be possible with mapping alone. Therefore, we investigate promising self-supervision signals for open-world class-incremental learning.

Based on the motivation to deploy robots to human environments, we focus this work on indoor scenes. Given a trajectory in the unknown environment, the robot collects observations with a RGB-D sensor in different modalities. These

encompass (1) predictions of the base segmentation model and their uncertainties, (2) deep features of the segmentation network and other image-based networks, (3) a volumetric map of the environment, and (4) geometric features extracted from that map. Subsequently, we categorize these observations through clustering and integrate everything back into the semantic segmentation network by training it with pseudo-labels. We obtain an updated network that can identify novel semantic categories and has overall higher prediction accuracy in the environment, as shown in Figure 1. In summary, our contributions are:

- A novel framework to map, discover, represent, and integrate novel objects into a semantic segmentation network in a self-supervised manner.
- An algorithm that leverages prior knowledge to optimise the clustering parameters for finding representations of novel objects.
- We provide the first open-source available method implementations and, while not at the scale of a benchmark, develop metrics and evaluation scenarios for open-world semantic scene understanding.

2 Related Work

Novel object discovery describes an algorithm’s ability to account for unknown object classes in perception data. Grinvald et al. [7] showed a semantic mapping framework that was able to segment parts of the scene as ‘unknown object’, but without the ability to categorize these. Nakajima et al. [9] were one of the first to demonstrate semantic scene understanding that can identify novel objects. They rely on superpixel segmentation, mapping, and clustering to identify object categories. Hamilton et al. [10] showed fully unsupervised video segmentation based on a similar framework like the one we describe in Section 3.1. Both [9] and [10] cluster a whole scene into semantic parts without the ability to relate a subset of clusters to known labels. Uhlemeyer et al. [11] recently demonstrated that based on advancement in out-of-distribution detection, a segmentation can be split into inliers and outliers. They cluster only the outliers into novel categories, but based on features that were already supervised on some of their outlier classes. In contrast to our method, theirs is therefore not fully unsupervised and further lacks the capability to integrate multiple observation modalities.

Clustering for classification can be understood as a two part problem. First, (high dimensional) descriptors for the items in question have to be found. Then, a clustering algorithm groups similar descriptors together. The established approach in representation learning is to learn a single good descriptor that can be clustered with kNN or k-means [12]. K-means can be used with mini-batches, is differentiable, fast, and easy to implement. However, we argue that there are two big disadvantages: it requires a priori knowledge of the number of clusters k and only works in the space of a single descriptor. For a scenario in which a robot is deployed to unknown environments, it cannot know the number of novel object categories. It is also questionable whether a single descriptor will be able to well describe all parts of the unknown environment. Graph clustering algorithms

like DBSCAN [13] or HDBSCAN [14] can cluster arbitrary graphs and do not need to know the number of clusters beforehand. Their hyperparameters are instead related to the values of the connectivity matrix. These graph edges are independent of any specific descriptor space and can e.g. also be an average over multiple descriptor distances. This makes graph clustering a better candidate when working with more than one descriptor (in clustering literature, this is called ‘multi-view’ clustering [15], which however is a very ambiguous term in scene understanding). Unfortunately, there exist no differentiable graph clustering algorithms. The closest in the literature is [16], which however links nodes to a single descriptor. [17] proposes a differentiable multi-descriptor clustering, which however just uses representation learning to link from multiple to one descriptor. Our work therefore investigates how graph clustering can be used to cluster scenes based on multiple descriptors. We further investigate how parameters of graph clustering can be tuned without gradient based optimisation.

Continual learning describes the problem of training a single model over a stream of data that e.g. contains increasing amount of classes, shifts in data distribution, etc. New knowledge should be integrated into the model without forgetting old knowledge. Prior work [8], [11] has already shown the effectiveness of pseudo-labels in continual learning and other works [18], [19] showed techniques for supervised class-incremental semantic segmentation that mitigate forgetting. However, supervision is not available in autonomous open-world operation. We therefore focus this work on the self-supervision part of class-incremental learning, while referring to [18], [19] for ways to address or evaluate forgetting.

3 Method

In the following we define the problem of open-world scene understanding. We first take a step back and set up a general formal description of the problem, which we show relates to similar works on segmentation, and enables us to identify the core differences between the evaluated methods. We then describe how we identify novel object categories, and how we use this identification to train the robot’s segmentation network in a self-supervised manner.

3.1 Preliminaries: Scene Understanding as a Clustering Problem

A robot explores an environment and collects over its trajectory camera images and consequently through simultaneous localisation and mapping (SLAM) corresponding poses in relation to the built map.

Let $G = (V, E)$ describe a graph where every vertex $v_i \in V$ is an observed pixel, as illustrated in Fig. 2. For each of these observation vertices v_i , the following information is available:

- image plane coordinates in the corresponding camera image
- 3D coordinates $T_{\text{map} \rightarrow v_i}$ in the robot map
- time of observation $t(v_i)$

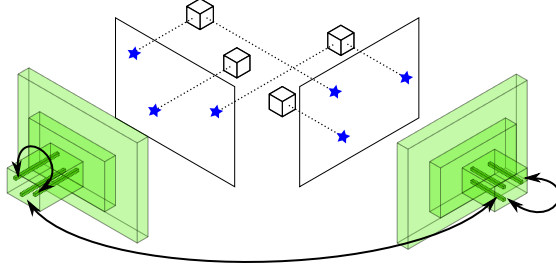


Fig. 2: Illustration of the graph setup. Every node (star) is a pixel in a camera frame. For every node, we also know the projection into 3D and potential correspondences from other frames. We can further relate nodes within and between frames through deep features from networks run on the frames.

- semantic prediction $\text{pred}(v_i)$ and associated (un)certainty $\text{cert}(v_i)$
- any local visual / learned / geometric feature $f(v_i)$ that can be inferred from the corresponding camera image, map location, or additional sensing modalities available on the robot

Edges can then in general be found from a function $e : V \times V \rightarrow \mathbb{R}_{\geq 0}$:

$$e(v_i, v_j) = e(T_{v_i \rightarrow v_j}, \langle f(v_i), f(v_j) \rangle, \langle t(v_i), t(v_j) \rangle, \langle \text{pred}(v_i), \text{pred}(v_j) \rangle)$$

that, based on distance functions $\langle \cdot, \cdot \rangle$, distills the multimodal relations of v_i and v_j into an edge weight.

The semantic interpretation of the scene can then be expressed as the graph clustering problem on G that splits into disjoint clusters V_k .

$$V = \bigcup_{K \text{ clusters}} V_k \quad \forall i, j, i \neq j : V_i \cap V_j = \emptyset$$

The formulation above is very related to conditional random fields (CRFs) and the unsupervised segmentation loss from Hamilton et al. [10]. They show that this graph structure represents a Potts problem [20]. Briefly summarised: If $\phi : V \rightarrow \mathcal{C}$ (softly) assigns vertices to clusters and $\mu : \mathcal{C} \times \mathcal{C} \rightarrow \mathbb{R}$ sets a cost for the comparison between two assignments, e.g. the cross-entropy, the graph clustering problem introduced above minimizes the following energy term:

$$E(\phi) = \sum_{v_i, v_j \in V} e(v_i, v_j) \mu(\phi(v_i), \phi(v_j))$$

In the most simple case of perfect (i.e. ground-truth) predictions,

$$e(v_i, v_j) = \begin{cases} \text{const.} & \text{if } \text{pred}(v_i) = \text{pred}(v_j) \\ 0 & \text{otherwise} \end{cases}$$

is a disjoint graph with each cluster matching one label.

Often however, predictions are not perfect and techniques like volumetric semantic mapping can be used to filter noisy predictions by enforcing that a voxel

should have the same class regardless of the viewpoint. This roughly corresponds to the problem of clustering G with e.g.

$$e(v_i, v_j) = \begin{cases} 1 & \text{if } v_i, v_j \text{ in same voxel} \\ < 1 & \text{if } \text{pred}(v_i) = \text{pred}(v_j) \\ 0 & \text{otherwise} \end{cases}$$

where some approaches also take uncertainty or geometry into account.

3.2 Identifying Novel Categories

To identify novel categories in a scene, observation vertices v_i need to be clustered based on commonalities that go beyond position in the map and prediction of a pretrained classifier, because by definition the pretrained classifier will not be able to identify novel categories. As the predominant current approach in category prediction is to identify categories visually, we also follow this approach to cluster observations into novel categories based on a range of visual descriptors. In the above introduced graph clustering framework, this means:

$$e_{\text{ours}}(v_i, v_j) = \sum_{d \in \text{descriptors}} w_d \langle f_d(v_i), f_d(v_j) \rangle \quad (1)$$

with w_d the weight for each descriptor and $\sum w_d = 1$. Note that equation (1) is a generalisation of different related work. For example, Uhlemeyer et al.[11] links observations only by the feature of an Imagenet pretrained ResNet and Nakajima et al. [9] weight features from the pretrained segmentation network and geometric features based on the entropy of the classification prediction $h(v_i)$.

$$\begin{aligned} e_{\text{uhlemeyer}}(v_i, v_j) &= \|\text{tSNE}(\text{PCA}(f_{\text{imgnet}}(v_i))) - \text{tSNE}(\text{PCA}(f_{\text{imgnet}}(v_j)))\|_2 \\ e_{\text{nakajima}}(v_i, v_j) &= \|(1 - h(v_i))f_{\text{segm}}(v_i) - (1 - h(v_j))f_{\text{segm}}(v_j)\|_2 \\ &\quad + \|h(v_i)f_{\text{geo}}(v_i) - h(v_j)f_{\text{geo}}(v_j)\|_2 \end{aligned}$$

where $\text{tSNE}(\text{PCA}(\cdot))$ is a dimensionality reduction as described in [11].

Optimisation of Clustering Parameters

To solve the clustering problem of $G(V, E)$, different hyper parameters Θ have to be found. This includes parameters of the clustering algorithm and the weights w_d of the different descriptors. The choice of these parameters governs the ‘grade of similarity’ that is expected within a cluster, i.e. how fine-grained categories should be. In general, choosing these parameters is very hard because the choice has to hold for unknown objects and scenes. In this work, we therefore propose to solve the parameter choice by optimisation. In particular, we propose to use the subset $\tilde{V} \in V$ of observations where the prediction $\text{pred}(v)$ out of one of the known classes $1, \dots, K$ has high certainty $\forall v \in \tilde{V} : \text{cert}(v) > \delta$ and find the hyperparameters Θ as follows:

$$\Theta = \underset{v \in \tilde{V}}{\text{argmax}} \text{mIoU}(\{V_1, \dots, V_K\}, \{\text{pred}(v) = 1, \dots, \text{pred}(v) = K\}) \quad (2)$$

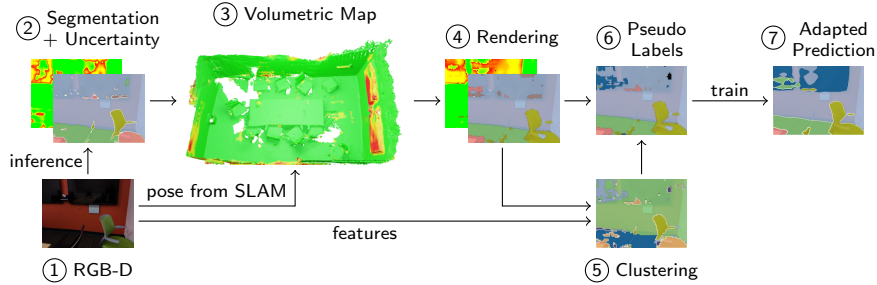


Fig. 3: Overview of the steps for self-supervised, class-incremental learning. The method is described in Section 3.2 and implementation details in Section 4.1.

where mIoU is the mean intersection over union (IoU) of the best matching between the clustering $\{V_1, \dots, V_K\}$ and the predictions of the pretrained classifier.

As shown in Section 2, there exists no graph clustering algorithm that is differentiable either to its input or its parameters. Eq. (2) is therefore not optimisable based on gradients. Hence, we employ black-box optimisation that models the clustering algorithm as a gaussian process $\Theta \rightarrow \text{mIoU}$. Based on the ‘skopt’ library [21], samples of Θ are chosen to cover the optimisation space but favoring areas where good mIoU is expected based on previous measurements. After 200 iterations, we select the point with the best mIoU.

Subsampling of the Clustering Graph

Usually $G(V, E)$ is too large to efficiently compute the clustering problem. With an already low image resolution of 640x480 and a frame rate of e.g. 20Hz, 2 min of camera trajectory correspond to $|V| > 7e9$. We therefore rely on random subsampling, taking 100 random points on every 5th frame, to create a smaller problem that is still representing the whole scene. Such subsampling removes redundancies in observations of neighboring pixels and subsequent frames, but also exaggerates noise that would otherwise average out over more data points. We hence choose parameters to the maximum possible with the available memory.

Subsampling however comes with the challenge that there is no direct clustering solution for all $v \in V$. We therefore combine the subsampled graph clustering with nearest neighbor search. Given a clustering for a subsampled part of V , we assign every v either to its cluster, if it was part of the graph clustering, or to the cluster of the nearest neighbor according to $e_{\text{ours}}(v_i, v_j)$.

Note that prior work reduces computationally complexity by first segmenting the scene into superpixels or segments and then clustering these. This approach comes with other challenges, notable how to attribute features to segments and how to ensure segments are not merging independent objects. With our subsampling, we test an alternative approach.

Self-Supervised Class-Incremental Training

To adapt the robot’s perception to a novel scene, on both known and unknown categories, we leverage the above described method as part of a larger system

that is outlined in Figure 3. Its goal is to produce a useful learning signal without any supervision, i.e. purely based on the observations the robot makes itself ①. With such a learning signal, we finetune the base segmentation model ② with the goal of improving the predictions in the given scene on the next trajectory.

As a volumetric mapping framework ③, we use the implementation from [22] without the panoptic part. This framework performs volumetric mapping and integration of semantic predictions per voxel. We extend this framework to also integrate uncertainties associated with the predictions as average per voxel. For pose-estimation, we rely on the poses provided with the data, which are obtained through visual-inertial mapping and bundle adjustment [23].

Because the semantic map integrates many predictions from different view-points, it cancels out some noise from single frame predictions and has a higher overall accuracy. This was used in [24] as a learning signal for scene adaptation, but assuming that all classes are known. Similar to [24], we also render ④ the semantic map back into each camera pose, obtaining an improved semantic prediction for every frame. We additionally render the averaged uncertainty, which indicates which parts of the scene are reliable predictions on inlier classes (low average uncertainty) and which parts are either novel categories or unfamiliar known categories (both high uncertainty), as shown in Figure 5.

Given a clustering solution ⑤, we produce pseudo-labels for training by merging renderings from the semantic map with clustering-based predictions ⑥. We first identify clusters with large overlap to predicted categories by measuring the contingency table between the semantic classes in the map and the clustering. We merge clusters that have an IoU $> .5$ with the corresponding predicted class. All other clusters are considered novel categories. We then assign for each pixel in each camera frame, i.e. each v_i , either (i) the rendered semantic class from the map if the average map uncertainty is below a threshold δ or (ii) the assigned cluster if the uncertainty of the prediction is higher than δ . Essentially, our pseudolabels therefore identify unknown parts of a scene and produce a learning signal to perform domain adaptation for the known parts of the scene and novel object discovery for the unknown parts of the scene.

To train the model on the pseudo labels ⑦, we need to extend its last layer to accommodate the newly identified categories. We do this by increasing the kernel and bias of the last layer from $\mathbb{R}^{F \times C}$ to $\mathbb{R}^{F \times (C+C')}$ where F is the feature size, C is the number of known classes, and C' is the number of novel detected clusters. We then initialise these matrixes with standard random initialisation for the new rows and with the base model’s parameters for the already existing rows.

4 Experimental Evaluation

We investigate the setting where a robot is put into a new environment that contains objects it has never seen. We choose the ScanNet dataset [23] of RGB-D trajectories in real indoor environments. Despite multiple errors in the semantic annotations, ScanNet had the highest data quality when we searched for datasets containing RGB-D trajectories, poses, and semantic annotations. The dataset

is split into scenes (usually one room), where each scene may include multiple trajectories. We select television, books, and towel as outlier classes, which the segmentation models must not have seen during training. After data quality filtering to e.g. account for incorrect annotations, we end up with 3 scenes with TVs, 1 scene with books and 2 scenes with towels (out of the first 100 validation scenes). Compared to prior work that tests on a total of 360 images [9] and 951 images [11], we therefore test on significantly more data with total of 15508 frames and at least 1000 frames per trajectory.

4.1 Method Implementation

We run two variants of our method: One is only taking self-supervised information as input, i.e. features of the segmentation network itself, self-supervised visual features from DINO [12], and geometric features. The second variant (following [11]) is also fusing visual information of a ResNet101 trained on Imagenet as input. Imagenet features are obtained by supervised training on a wide range of classes, including the ones we consider as outliers in our experimental setting, so they cannot be considered self-supervised.

We obtain geometric features by running the provided model of [25], which trains a descriptors to register 3D point clouds, on the surface point cloud of the voxel map. We extract features of our segmentation network at the ‘classifier.2’ layer, which is one layer before the logits. As Imagenet features, we take the output of the last ResNet block before flattening, such that the features still have spatial information (‘layer4’ in pytorch). From DINO, we take the last token layer that still has spatial relations. We normalise these descriptors to a l2 norm of 1 and calculate pairwise euclidean distances. We then harmonize the scale of different feature distances by finding scalar factors α such that $p(\alpha * |v_i - v_j| < 1) = .9$ for v_i, v_j that have low uncertainty and the same predicted class.

For clustering, we use HDBScan [14]. This is an improved version of DBScan that is designed to deal better with changing densities of the data and we found it in general to perform slightly more reliable.

As segmentation network, we use a DeepLabv3+ trained on COCO and then on ScanNet, but not on the scenes or objects categories we test on. We employ standard image augmentation and random crops. For uncertainty estimation, we take the method with the best simplicity-performance trade off from the Fishyscapes benchmark [26]: We use the max-logit value of the softmax, including the post-processing introduced in [27], but without their standardisation step.

4.2 Adaptation of Baselines

In addition to the full optimisation based approach above, we want to test concepts from related work. Unfortunately, neither [9] nor [11] made their implementation available, which is why we implement both methods and adapt them to our evaluation setting. It is important to note that these are not direct replications or reproductions, but we take as many ideas from these papers as possible and combine them with the system above to get the best result.

For Nakajima et al. [9], we implement their clustering procedure, but take the same segmentation network, mapping framework, and geometric features as for our method. Since we could not find all clustering parameters in their paper, we run our proposed parameter optimisation on the inflation and η parameter of the MCL clustering for every scene. Because MCL takes longer than HDBScan, we needed to use stronger subsampling. Given that our geometric features are very different than the ones used in [9], we also evaluate a variant that only uses the features of the segmentation network. In [9], this had slightly worse performance.

For Uhlemeyer et al. [11], their underlying meta-segmentation is released as open-source. However, their uncertainty estimation is only available for an urban driving network, so we replace it with the uncertainty metric that we also use for our method. Also this paper does not report its clustering parameters. We however cannot run our proposed parameter optimisation for this method, because it only clusters the outliers. We therefore, following advice of the authors, hand-tune the parameters until we get a good result for scene 0354 and use these settings ($\epsilon = 3.5$, min samples = 10) for all scenes.

4.3 Evaluation Metrics

The evaluation protocol in prior work is not well documented [9] or limited to one novel cluster [11]. We therefore describe our protocol in more detail. Class-incremental learning is usually supervised and therefore evaluated with a standard confusion matrix [28]. In unsupervised representation learning literature, the number of clusters is usually set to the number of labels, such that the Hungarian Algorithm can find the optimal matching of clusters and labels [10], [12].

In our problem setting, these assumptions do not hold. Parts of the predicted classes are trained in a supervised manner and only the novel categories are found in an unsupervised way. Because parts of the scenes contain outlier objects without annotation, we can also not punish a method for finding more categories than there are labels. To match clusters to existing labels, we first count how often which cluster is predicted for which label in the contingency matrix of size $N_{\text{labels}} \times N_{\text{clusters}}$ on the labelled part of the scene. We then use a variant of the Hungarian algorithm [29] that first pads the matrix with zeros to a square matrix and further disallows to assign predictions with a supervised label to another label (they may however be disregarded entirely if an unlabelled cluster is a better match). If no prediction has a supervised label, this is equivalent to the established Hungarian matching from representation learning. If all predictions have supervised labels, this is equivalent to the standard confusion matrix.

We also report the v-score [30], which is independent of label-cluster matching. It is the harmonic mean over two objectives: All points in a cluster belong to the same label, and all predictions of a label come from the same cluster.

4.4 Results

We present the main results of this study in Table 1. Qualitative examples can be found in the video attachment. In general, we observe that all methods are



Fig. 4: Predictions on unlabelled parts of the scene reveal that the adapted network detects more novel classes than the labels allow to measure.

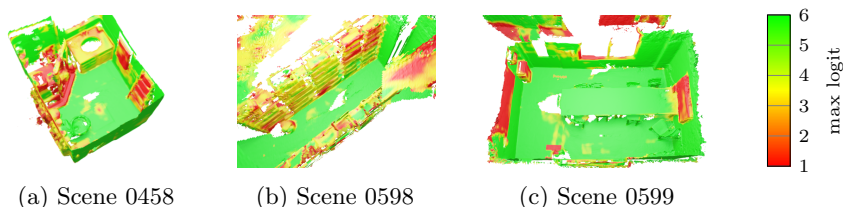


Fig. 5: Uncertainty in the volumetric maps, measured as the max-logit (lower is more uncertain). As expected, the outlier objects towel (a), books (b), and TV (c) have high uncertainty. Note that some other objects like the ladder in (a) that is also shown in Figure 4 have high uncertainty.

able to detect the novel object categories to a certain degree, except for variants of nakajima in scene 0598. We also observe that the full nakajima variant with segmentation and geometric features performs poorly, but note that the method was originally designed for different geometric features and the segmentation-only variant performs much better.

Those methods that adapt the segmentation model through training (ours and uhlemeyer) in all cases improve performance over the base model. Where a second trajectory of the environment is available, we can also verify that this is a true improvement of the segmentation and not overfitting on the frames. Notably, our fully unsupervised variant⁴ is better than all supervised methods in 2 scenes and competitive in the other scenes. This indicates that the use of supervised ImageNet pretraining is limited and very useful features can instead be learned unsupervisedly from any environment in open-world deployment.

As discussed in Section 2, graph clustering does not require a priori knowledge of the number of classes. As such, Figure 4 shows examples of objects that are not measurable as outliers, yet got discovered by the algorithms and predicted as a new category by the trained network.

In scenes like 0568 or 0164, no investigated approach is able to discover the outlier class. Especially small objects and cluttered scenes pose big challenges.

We conclude that our approach that is fusing multiple sources of information, especially the unsupervised variant, shows the most consistent performance over the listed scenes, but there is no approach that is the best in every scene.

⁴ ‘unsupervised’ refers to novel classes. All tested methods are supervised on the known classes.

outlier scene method		training traj.		new traj.		
		out	mIoU	out	mIoU	
tv	0354	base model	0	47	-	-
		adapted nakajima: segm. + geom.	7	4	-	-
		adapted nakajima: segm. only	9	20	-	-
		SCIM fusing segm. + geom. + dino	73	62	-	-
		adapted uhlemeyer: imgn.	65	60	-	-
		adapted uhlemeyer: imgn. + map	21	56	-	-
		SCIM fusing segm. + geom. + imgn.	41	54	-	-
tv	0575	base model	0	53	0	53
		adapted nakajima: segm. + geom.	10	11	-	-
		adapted nakajima: segm. only	24	17	-	-
		SCIM fusing segm. + geom. + dino	33	64	39	63
		adapted uhlemeyer: imgn.	12	55	23	61
		adapted uhlemeyer: imgn. + map	6	62	4	58
		SCIM fusing segm. + geom. + imgn.	50	69	28	63
tv	0599	base model	0	60	0	63
		adapted nakajima: segm. + geom.	1	0	-	-
		adapted nakajima: segm. only	36	26	-	-
		SCIM fusing segm. + geom. + dino	37	67	36	63
		adapted uhlemeyer: imgn.	42	71	55	74
		adapted uhlemeyer: imgn. + map	11	70	10	68
		SCIM fusing segm. + geom. + imgn.	32	65	31	62
books	0598	base model	0	59	-	-
		adapted nakajima: segm. + geom.	1	1	-	-
		adapted nakajima: segm. only	0	0	-	-
		SCIM fusing segm. + geom. + dino	43	77	-	-
		adapted uhlemeyer: imgn.	29	63	-	-
		adapted uhlemeyer: imgn. + map	29	70	-	-
		SCIM fusing segm. + geom. + imgn.	33	74	-	-
towel	0458	base model	0	48	0	38
		adapted nakajima: segm. + geom.	6	7	-	-
		adapted nakajima: segm. only	63	44	-	-
		SCIM fusing segm. + geom. + dino	33	57	37	47
		adapted uhlemeyer: imgn.	38	61	47	49
		adapted uhlemeyer: imgn. + map	38	59	46	48
		SCIM fusing segm. + geom. + imgn.	60	63	79	55
towel	0574	base model	0	45	-	-
		adapted nakajima: segm. + geom.	22	7	-	-
		adapted nakajima: segm. only	4	27	-	-
		SCIM fusing segm. + geom. + dino	28	52	-	-
		adapted uhlemeyer: imgn.	23	50	-	-
		adapted uhlemeyer: imgn. + map	f	f	-	-
		SCIM fusing segm. + geom. + imgn.	39	53	-	-

Table 1: Model predictions in [% mIoU] for different scenes and different outlier classes. We mark the best unsupervised method and the best overall. The available unsupervised information are the base model’s features (segm.), geometric features (geom.), and DINO [12] features (dino). Some methods however use features from supervised ImageNet training (imgn.). Note that ‘nakajima’ is a pure clustering method, so we measure the clustering instead of model predictions. For those scenes where a second trajectory is available, we evaluate trained models on the second trajectory.

variant	information				single class IoU							mIoU v score		
	3D	segm	imgn	geom	wall	floor	chair	table	door	window	tv	whiteboard		
base model	-	-	-	-	81	72	67	84	30	12	0	30	47	62
semantic map	✓	-	-	-	82	78	73	89	33	8	0	51	52	68
clustering	seg only	-	1	-	-	51	5	11	3	0	0	28	12	27
	seg + imgn	-	.69	.31	-	32	32	47	27	10	1	27	23	40
pseudolabel	seg only	✓	1	-	-	83	78	73	91	37	21	42	56	68
	seg + imgn	✓	.69	.31	-	84	78	73	91	37	19	43	56	69

Table 2: Ablation of different information sources on scene 0354.00. Listed in ‘information’ are the weights of different feature distances.

variant	information				single class IoU							mIoU v score		
	3D	segm	imgn	geom	wall	floor	cabinet	door	mirror	ceiling	towel	sink		
base model	-	-	-	-	53	76	76	18	10	61	0	62	45	56
semantic map	✓	-	-	-	50	83	77	11	14	60	0	57	44	59
clustering	seg only	-	1	-	-	37	33	0	0	0	0	0	9	25
	seg + geo	-	.94	-	.06	23	31	71	26	22	19	12	19	28
	seg + imgn + geo	-	.64	.15	.21	31	22	0	11	0	0	0	8	23
pseudolabel	seg only	✓	1	-	-	43	80	50	11	0	58	4	84	41
	seg + geo	✓	.94	-	.06	48	80	72	11	23	58	16	84	49
	seg + imgn + geo	✓	.64	.15	.21	48	80	50	11	5	58	32	84	46

Table 3: Ablation of different information sources on scene 0574.00. Listed in ‘information’ are the weights of different feature distances.

4.5 Design Choice Verification

We now evaluate different design choices. In Figure 5, we show the volumetric maps of different environments and the mapped uncertainty estimation. These maps show that the uncertainty in combination with mapping is very effective to identify uncertain parts of the scene. Next to the ‘target’ objects, also other uncertain objects are identified. It is expected that a model can also be uncertain about known classes, or that more than 1 novel object are present in a scene. We further show this in Figure 4.

As described in Section 3.2, we choose clustering parameters based on an optimisation objective. Figure 6 shows an analysis of whether this objective, which only approximates the true clustering performance, correlates with the true performance of the clustering. For this analysis, we subsample every 20th frame and cluster segmentation features only, to then evaluate the full clustering performance at every 5th optimisation step. We observe that the correlation increases in noise for higher mIoU, but in general correlates well enough to disregard bad parameters.

Tables 2 and 3 investigate how beneficial multiple sources of information are in the clustering problem. Firstly, the tables show that clustering with the segmentation features does not result in the same performance as the prediction of the same network, indicating that significant knowledge about classes is stored in the final layer (we extract features before the final layer). Over both scenes, we see that multiple sources of information result in better pseudolabels than just the segmentation features. We also see that which information is useful differs from scene to scene, motivating our decision to select the weights of the sources in

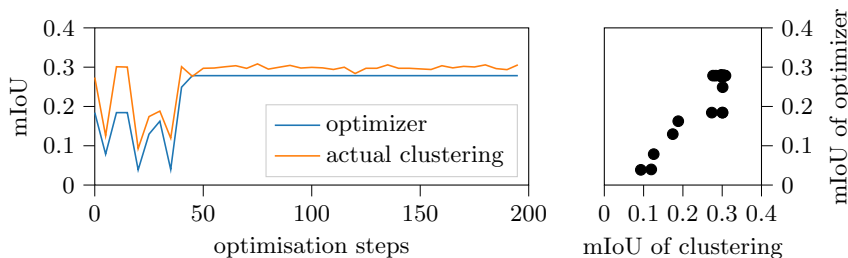


Fig. 6: Analysis of the correlation between the optimisation objective (clustering subset measured against high-confidence predictions) and the actual performance of the clustering (full images measured against ground-truth labels).

each scene through optimisation. While the combination of all features therefore creates a robust clustering for different scenes, Table 3 shows that this can result in a small tradeoff in single scene performance. We assume that this is caused by the increase of the optimisation space for every new feature.

5 Discussion & Outlook

We investigate the problem of semantic scene understanding in unknown environments containing novel objects. We develop a framework of clustering, inference, and mapping that can be used to autonomously discover novel categories and improve semantic knowledge. It generalises over existing work and helps us to create a new method based on black-box optimisation and information fusion.

To discover novel categories, our experiments show that unsupervised features are as useful as supervised ones, especially when multiple features are used. We also show that prior knowledge is very helpful, e.g. to optimize parameters. Better (gradient based) optimisation and a less noisy objective function may even improve this mechanism. In general, from the components in Figure 3, most are able to propagate gradients, opening opportunities for future research to replace more heuristics with deep learning.

While we showed that information fusion can be advantageous, it requires graph clustering, which is neither mini-batch compatible nor differentiable. We do not report runtimes, because all steps after mapping are not required to be online and our implementations are not optimised for this. We can however report that the meta segmentation of [11] and our optimisation usually required multiple hours. Both points show the potential of more efficient clustering.

This work did not touch upon the questions of continual learning or active exploration. The first asks how to organise class-incremental learning such that more and more semantic categories can be discovered as a robot moves from scene to scene. Prior work as touched on this topic [8], [11], [19], but none has evaluated self-supervised approaches with multiple classes over multiple consecutive environments. Similarly, the influence of actively planning trajectories to aid discovery remains to be investigated, with promising results from domain adaptation on known classes indicating that planning is helpful [31], [32].

Our experiments had to overcome a lack of available implementations and quality problems in the data. By releasing our segmentation models, implementations of related work, and implementation of our SCIM approach, we aim to accelerate future research on this topic.

References

- [1] S. Garg, N. Sünderhauf, F. Dayoub, D. Morrison, A. Cosgun, G. Carneiro, Q. Wu, T.-J. Chin, I. Reid, S. Gould, P. Corke, and M. Milford, “Semantics for Robotic Mapping, Perception and Interaction: A Survey,” English, *Foundations and Trends® in Robotics*, vol. 8, no. 1–2, 2020.
- [2] B. Liu, “Learning on the Job: Online Lifelong and Continual Learning,” *AAAI*, vol. 34, no. 09, 2020.
- [3] K. J. Joseph, S. Khan, F. S. Khan, and V. N. Balasubramanian, “Towards Open World Object Detection,” 2021.
- [4] J. Cen, P. Yun, J. Cai, M. Y. Wang, and M. Liu, “Deep Metric Learning for Open World Semantic Segmentation,” 2021.
- [5] M. Lungarella, G. Metta, R. Pfeifer, and G. Sandini, “Developmental robotics: A survey,” *Connection Science*, vol. 15, no. 4, 2003.
- [6] J. McCormac, A. Handa, A. Davison, and S. Leutenegger, “SemanticFusion: Dense 3D Semantic Mapping with Convolutional Neural Networks,” *Bayesian Forecasting and Dynamic Models*, vol. 22, no. 2, 2016.
- [7] M. Grinvald, F. Furrer, T. Novkovic, J. J. Chung, C. Cadena, R. Siegwart, and J. Nieto, “Volumetric Instance-Aware Semantic Mapping and 3D Object Discovery,” *IEEE Robotics and Automation Letters*, vol. 4, no. 3, 2019.
- [8] H. Blum, F. Milano, R. Zurbrügg, R. Siegwart, C. Cadena, and A. Gawel, “Self-Improving Semantic Perception for Indoor Localisation,” en, in *Proceedings of the 5th Conference on Robot Learning*, 2021.
- [9] Y. Nakajima, B. Kang, H. Saito, and K. Kitani, “Incremental Class Discovery for Semantic Segmentation with RGBD Sensing,” 2019.
- [10] M. Hamilton, Z. Zhang, B. Hariharan, N. Snavely, and W. T. Freeman, “Unsupervised Semantic Segmentation by Distilling Feature Correspondences,” en, in *ICLR*, 2022.
- [11] S. Uhlemeyer, M. Rottmann, and H. Gottschalk, “Towards Unsupervised Open World Semantic Segmentation,” 2022.
- [12] M. Caron, H. Touvron, I. Misra, H. Jégou, J. Mairal, P. Bojanowski, and A. Joulin, “Emerging Properties in Self-Supervised Vision Transformers,” *arXiv:2104.14294 [cs]*, 2021.
- [13] M. Ester, H.-P. Kriegel, and X. Xu, “A Density-Based Algorithm for Discovering Clusters in Large Spatial Databases with Noise,” en, 1996.
- [14] R. J. G. B. Campello, D. Moulavi, and J. Sander, “Density-Based Clustering Based on Hierarchical Density Estimates,” en, in *Advances in Knowledge Discovery and Data Mining*, J. Pei, V. S. Tseng, L. Cao, H. Motoda, and G. Xu, Eds., ser. Lecture Notes in Computer Science, 2013.

- [15] L. Fu, P. Lin, A. V. Vasilakos, and S. Wang, “An overview of recent multi-view clustering,” *Neurocomputing*, vol. 402, 2020.
- [16] S. A. Shah and V. Koltun, “Deep Continuous Clustering,” 2018.
- [17] S. Du, Z. Liu, Z. Chen, W. Yang, and S. Wang, “Differentiable Bi-Sparse Multi-View Co-Clustering,” *IEEE Trans. Signal Process.*, vol. 69, 2021.
- [18] L. Yu, X. Liu, and J. van de Weijer, “Self-Training for Class-Incremental Semantic Segmentation,” 2020.
- [19] U. Michieli and P. Zanuttigh, “Incremental learning techniques for semantic segmentation,” 2019.
- [20] R. B. Potts, “Some generalized order-disorder transformations,” en, *Mathematical Proceedings of the Cambridge Philosophical Society*, 1952.
- [21] T. Head, M. Kumar, H. Nahrstaedt, G. Louppe, and I. Shcherbatyi, *Scikit-optimize/scikit-optimize*, 2021.
- [22] L. Schmid, J. Delmerico, J. Schönberger, J. Nieto, M. Pollefeys, R. Siegwart, and C. Cadena, “Panoptic Multi-TSDFs: A Flexible Representation for Online Multi-resolution Volumetric Mapping and Long-term Dynamic Scene Consistency,” in *ICRA*, 2022.
- [23] A. Dai, A. X. Chang, M. Savva, M. Halber, T. Funkhouser, and M. Nießner, “Scannet: Richly-annotated 3d reconstructions of indoor scenes,” in *CVPR*, 2017.
- [24] J. Frey, H. Blum, F. Milano, R. Siegwart, and C. Cadena, “Continual Learning of Semantic Segmentation using Complementary 2D-3D Data Representations,” *arXiv:2111.02156 [cs]*, 2021.
- [25] Z. Gojcic, C. Zhou, J. D. Wegner, and A. Wieser, “The Perfect Match: 3D Point Cloud Matching With Smoothed Densities,” in *2019 IEEE/CVF Conference on Computer Vision and Pattern Recognition (CVPR)*, 2019.
- [26] H. Blum, P.-E. Sarlin, J. Nieto, R. Siegwart, and C. Cadena, “The Fishyscapes Benchmark: Measuring Blind Spots in Semantic Segmentation,” en, *International Journal of Computer Vision*, vol. 129, no. 11, 2021.
- [27] S. Jung, J. Lee, D. Gwak, S. Choi, and J. Choo, “Standardized Max Logits: A Simple yet Effective Approach for Identifying Unexpected Road Obstacles in Urban-Scene Segmentation,” 2021.
- [28] A. Douillard, Y. Chen, A. Dapogny, and M. Cord, “PLOP: Learning without Forgetting for Continual Semantic Segmentation,” 2020.
- [29] *Munkres — Munkres implementation for Python.*
- [30] A. Rosenberg and J. Hirschberg, “V-Measure: A Conditional Entropy-Based External Cluster Evaluation Measure,” in *Joint Conference on Empirical Methods in Natural Language Processing and Computational Natural Language Learning (EMNLP-CoNLL)*, 2007.
- [31] R. Zurbrügg, H. Blum, C. Cadena, R. Siegwart, and L. Schmid, “Embodied Active Domain Adaptation for Semantic Segmentation via Informative Path Planning,” arXiv, Tech. Rep. arXiv:2203.00549, 2022.
- [32] D. S. Chaplot, M. Dalal, S. Gupta, J. Malik, and R. R. Salakhutdinov, “SEAL: Self-supervised Embodied Active Learning using Exploration and

3D Consistency,” in *Advances in Neural Information Processing Systems*, vol. 34, 2021.

A Qualitative Examples

We show qualitative examples in Figures 7 and 8.

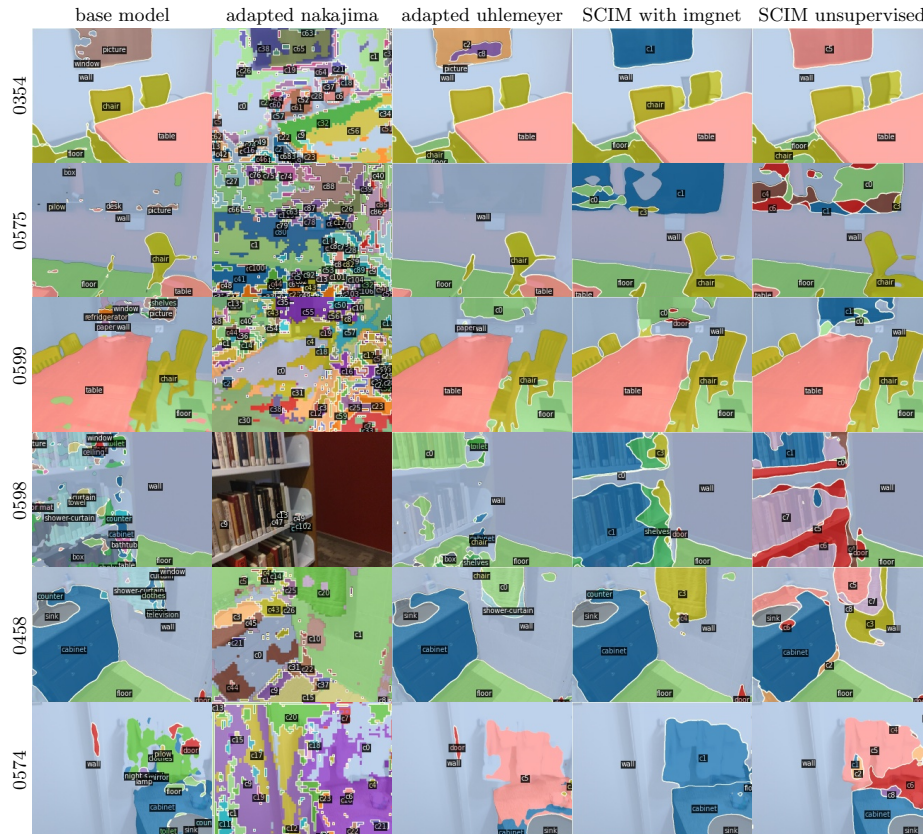


Fig. 7: Qualitative examples corresponding to the results in Table 1.

B Selection of Evaluation Scenes

We download the first 100 validation scenes of ScanNet and find in there 6 scenes with television, 5 scenes with towel and 4 scenes with books. To account for mistakes in the labelling and other data quality issues, we further had to filter them:

- We remove scenes 0426 and 0608 (both with tvs) because of too many novel objects without annotation and severe degradation of the base model performance (see Table 4).

outlier scene method			training traj. out IoU mIoU	
tv	0426	base model	0	36
		base model	0	50
		adapted nakajima, segm. only	9	31
tv	0568	SCIM fusing segm. + geom. + dino	0	52
		adapted uhlemeyer	0	53
		adapted uhlemeyer + map	0	60
		SCIM fusing segm. + geom. + imgn.	0	54
tv	0608	base model	0	45
books	0025	base model	0	42
		adapted uhlemeyer	0	44
		SCIM fusing segm. + geom. + imgn.	8	49
		base model	0	50
		adapted nakajima, segm. only	6	25
towel	0164	adapted uhlemeyer	12	48
		adapted uhlemeyer + map	0	53
		SCIM fusing segm. + geom. + imgn.	10	54

Table 4: Challenging Scenes in which no method achieves good detection of the outlier, often due to clutter.